Crystal structure transformations induced by surface stresses in BaTiO3 and BaTiO3@SiO2 nanoparticles and ceramics

V.V. Laguta[a,b]*, C. Elissalde[c], M. Maglione[c], A.M. Artemenko[a,c], V. Chlan[d], H. Štěpánková[d] and Yu. Zagorodniy[a]

[a]*Institute for Problems of Material Science, NASc, Kiev, Ukraine;* [b]*Institute of Physics ASCR, Prague, Czech Republic;* [c]*Institute of Condensed Matter Chemistry, Bordeaux, France;* [d]*Faculty of Mathematics and Physics, Charles University in Prague, Prague, Czech Republic*

Lattice structure transformations in nanopowders of ferroelectric $BaTiO_3$ and BaTiO3@SiO_2 core-shell nanostructured ceramics were studied by nuclear magnetic resonance (NMR) and electron paramagnetic resonance (EPR) at the temperatures 120−450 K and particle size of 300 and 500 nm. NMR spectra of all studied samples in the paraelectric phase are identical to the spectra in bulk material indicating their perfect perovskite structure without visible influence of particle surface. However, we have found that surface of particles essentially influence the ferroelectric phase transitions detected by both NMR and EPR techniques. The strongest changes as compared to bulk material were observed in BaTiO3@SiO_2 core-shell ceramics. Thorough analysis of NMR spectra suggests that the orthorhombic-like symmetry phase coexists here with other polar phases up to the Curie temperature. Depending on temperature, its relative volume varies from 25% to 100%. We assume that the orthorhombic-like symmetry phase is stabilized by anisotropic components of surface stresses which increase also global stability of polar state in nanoceramics to the temperature in bulk material. We summarize our results in a phase diagram.

Keywords: barium titanate; nanoparticles; ceramics; nuclear magnetic resonance; ferroelectric phase transition

1. Introduction

The current miniaturization in micro/nanoelectronics and telecommunications needs functional materials at nanometric scale. Barium titanate ($BaTiO_3$) is an important ferroelectric material used in the electronic industry due to its outstanding dielectric, piezoelectric and ferroelectric properties.[1] It undergoes three phase transitions when the temperature decreases from 394 to 175 K. Above 393 K, $BaTiO_3$ has cubic non-polar phase with space group $Pm\bar{3}m$. Between 393 and 268 K, the stable phase is polar tetragonal *P4mm*. At cooling to 267−268 K, the structure changes to the orthorhombic *C2mm*. Below 175 K, the stable phase has rhombohedral symmetry *R3m*.[2] All these transitions are first-order phase transitions. They show large temperature hysteresis, which is up to 29 deg. for the low-temperature orthorhombic-rhombohedral phase transition.

Currently, there are numerous publications in literature on investigation of the size-dependent phenomena in $BaTiO_3$ nanoparticles and nanograin ceramics.[3−8] In particular, it was shown theoretically [3,4] and experimentally [5−8] that the transition from the polar tetragonal (T) to non-polar cubic (C) phase takes place below the temperature T_C

*Correspondingauthor.Email:laguta@fzu.cz

which depends on the particle size and decreases down to room temperature at the particles, critical size from about 80 to 120 nm. This size-dependent phenomenon was explained by increasing influence of mechanical surface stresses and depolarization fields on stability of polar phase in a small ferroelectric particle due to large surface/volume ratio. In phenomenological approach, it can be considered as a surface tension.[4] However, a little is known about stability of other ferroelectric phases in nanoparticles and nanograined ceramics of $BaTiO_3$. We can mention here recent publication [8], which reports crystal structure transformation of $BaTiO_3$ nanopowders with the particle size from 5 up to 100 nm studied by high-resolution X-ray diffraction. In particular, the authors report about coexistence of different phases in the temperature range from 200 to 450 K and pay attention on importance of the shear stresses on the particle surface.

Recently $BaTiO_3$ [9] and (1-x)$BaTiO_3$-x$SrTiO_3$ [10,11] core-shell nanostructures were introduced in order to reduce dielectric losses at high frequencies in nanograin ceramics. In such nanostructures, the ferroelectric particles are isolated from each other by the dielectric shell, such as SiO_2 or Al_2O_3. Therefore, they keep their size during the densification process. This enables the production of ceramics with grain size control, which is usually not achieved with standard ceramic technology. An additional stress from the dielectric shell is expected in the core-shell nanostructure which can much more strongly change the ferroelectric properties of nanoparticles. On the other hand, such objects are very suitable for investigation of crystal structure transformations induced by surface stresses.

In the present paper, we investigated the surface tension and crystallite size dependent phenomena in $BaTiO_3$ nanoparticles with relatively large particle sizes from about 500 to 300 nm, where the ferroelectric phase transitions are still sharp and well seen. We also studied crystal structure transformations induced by surface stresses in the $BaTiO_3$ core-shell nanostructured ceramics prepared from the nanoparticles coated with amorphous SiO_2 or Al_2O_3. We used ^{137}Ba nuclear magnetic resonance (NMR) as a sensitive probe of the local structure of nanoparticles. This method does not need the long-range atomic ordering and therefore it allows relatively easy to distinguish different structural phases in small particles and their changes with the change of temperature and particles size. In addition, the electron paramagnetic resonance (EPR) of Mn^{2+} and Fe^{3+} paramagnetic ions was applied in the study of the low-temperature orthorhombic-rhombohedral phase transition at 120−220 K.

Our main finding is that even in the relatively large particles of $BaTiO_3$, with average size of 300 nm, there is marked influence of mechanical surface stresses on lattice parameters in vicinity of phase transitions, especially at low temperatures. In particular, the temperature interval stability of the tetragonal phase decreases. Contrary, the temperature interval stability of the orthorhombic phase essentially increases, especially in the $BaTiO_3$@SiO_2 core-shell composition. NMR data show that even relatively large particles of 300 nm in diameter contain regions of the orthorhombic-like symmetry at the temperatures which correspond to the nominal tetragonal and rhombohedral phases of $BaTiO_3$. The orthorhombic-like symmetry regions even prevail in the $BaTiO_3$@SiO_2 core-shell ceramics.

2. Experimental

$BaTiO_3$ powders with average diameter of particles 300 and 500 nm (hereafter in the text, BTO-500 and BTO-300) have been purchased from Sakai Chemical Industry Co., Ltd. Coating with amorphous SiO_2 (BTO@SiO_2 core-shell particles) was performed via the so-called Stöbber process. The coating procedure is described elsewhere.[9] Ceramic samples were prepared using conventional sintering at 900 °C in air. The $BaTiO_3$ powders

have relatively small distribution of particle size as can be seen from the scanning electron microscopy (SEM) photograph of BTO-300 powder shown in Figure 1(a). The SEM photograph of BTO-300@SiO_2 ceramics is shown in Figure 1(b). The ceramic is porous with grain size from about 0.3 up to 1 μm. Each grain contains from one to about five particles of $BaTiO_3$ coated by isolating SiO_2 shell.

The ^{137}Ba ($I = 3/2$, natural abundance 11.3%) NMR spectra were measured in a magnetic field $B_0 = 9.4$ T corresponding to a Larmor frequency ν_L at 44.479 MHz. A two $\pi/2$ pulse, four phase (xx, xy, x-x, x-y) 'exorcycle' phase sequence has been used to avoid echo signal distortions. The length of the $\pi/2$-pulse was typically $\sim$5 μs. The spectra were measured at the 120−410 K temperature range. The temperature stability and the precision of its measurement were better than 0.2 K.

EPR measurements were performed at standard spectrometer operating at frequency 9.2−9.4 GHz utilizing a TE_{102} rectangular microwave cavity with 100 kHz magnetic field modulation. The samples were sealed in quartz tube and placed in an Oxford Instruments ESR 900 continuous-flow helium cryostat inside the microwave cavity. The temperature could be varied and controlled over the temperature range 4−300 K with the accuracy of 0.2 K.

3. Experimental results and their interpretation

3.1. Tetragonal-orthorhombic phase transition

The ^{137}Ba NMR spectra measured at the temperature 292 K for micrograin ceramics, powders with particle sizes 500 and 300 nm and BTO-300@SiO_2 ceramics are presented in Figure 2.

For micrograin ceramics and the powder with larger particle size (500 nm), the shape of the spectrum is close to that expected for the tetragonal symmetry of Ba site in the tetragonal ferroelectric phase of $BaTiO_3$ (see, e.g. [12]). Only the $1/2 \leftrightarrow -1/2$ central transition perturbed by the second-order quadrupole interaction of the ^{137}Ba nuclei with the electric field gradients (EFG) is observed. However, with decrease of the particles size to 300 nm, the NMR lineshape markedly changes. In particular, an almost symmetrical line appears at the Larmor frequency (Figure 2(c)). This signals that in these particles, the lattice symmetry at the temperature 292 K differs from the pure *P4mm* tetragonal symmetry. ^{137}Ba NMR spectrum in BTO-300@SiO_2 ceramics undergoes even more

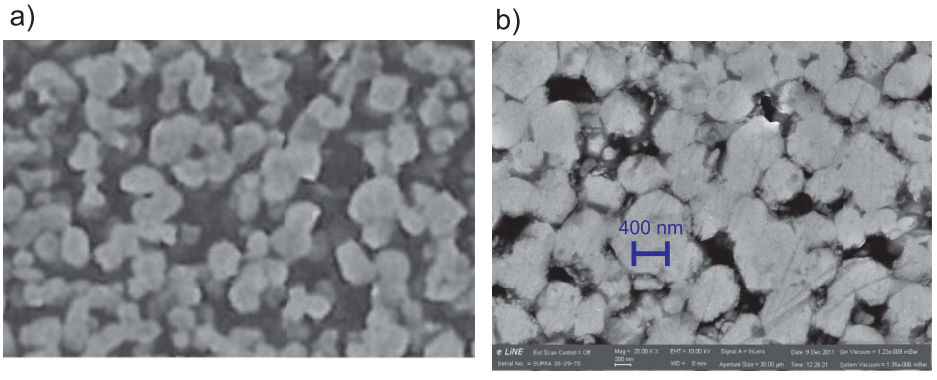

Figure 1. (a) Scanning electron microscopy photographs of BTO-300 powder with the mean particles size 300 nm and (b) BTO-300@SiO_2 ceramics shown at the same scale.

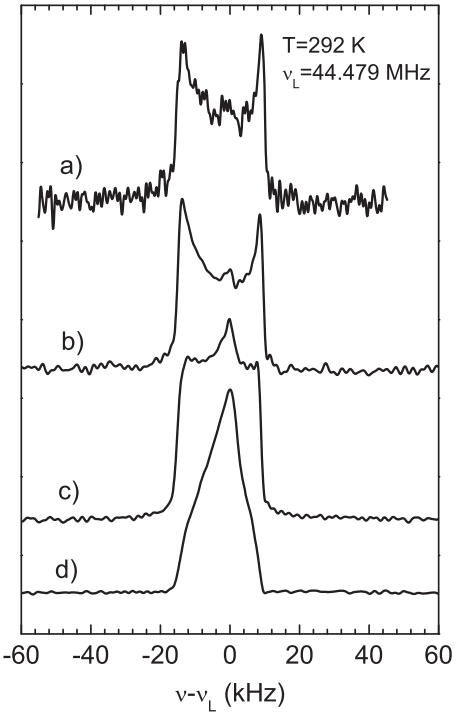

Figure 2. ^{137}Ba NMR spectra measured at 292 K in $BaTiO_3$: (a) normal micrograin ceramics; (b) BTO-500 powder; (c) BTO-300 powder; (d) BTO-300@SiO_2 ceramics.

drastic changes: singularities at the lineshape edges smear and the symmetrical component at the Larmor frequency essentially increases in intensity. This spectrum looks like the spectrum in the orthorhombic phase, [12] probably with small contribution of the tetragonal phase, created in large particles. Note that NMR spectrum in BTO-300@SiO_2 core-shell powder is practically the same as in BTO-300 nm powder. The change in the spectrum appears only after densification of the powder into ceramics.

The presence of the orthorhombic-like phase at the temperatures where formally there must be only the tetragonal phase is further supported by measurements in the vicinity of the tetragonal-orthorhombic phase transition temperature (Figure 3). One can see that in BTO-500 powder, the NMR lineshape changes at the temperature between 280 and 275 K that approximately corresponds to the temperature region of the tetragonal-orthorhombic phase transition in bulk material. But for smaller particles, this phase transition is markedly shifted to a higher temperature. It realizes between 288 and 280 K in BTO-300 (Figure 3(b)). However, BTO-300@SiO_2 ceramics remains in the orthorhombic phase at 295−300 K, almost 20 deg. higher than the phase transition temperature in bulk material. It mostly transforms into the tetragonal symmetry phase only at 330 K (Figure 3(c)), far from the phase transition temperature in bulk material. Starting from this temperature, the spectrum shape becomes similar to that in BTO-500 measured at 285 K (Figure 3(a)).

3.2. Tetragonal-cubic phase transition

Behaviour of ^{137}Ba NMR spectra in the vicinity of the tetragonal-cubic phase transition is shown in Figure 4. The NMR spectrum of all four samples, micrograin ceramics, powders

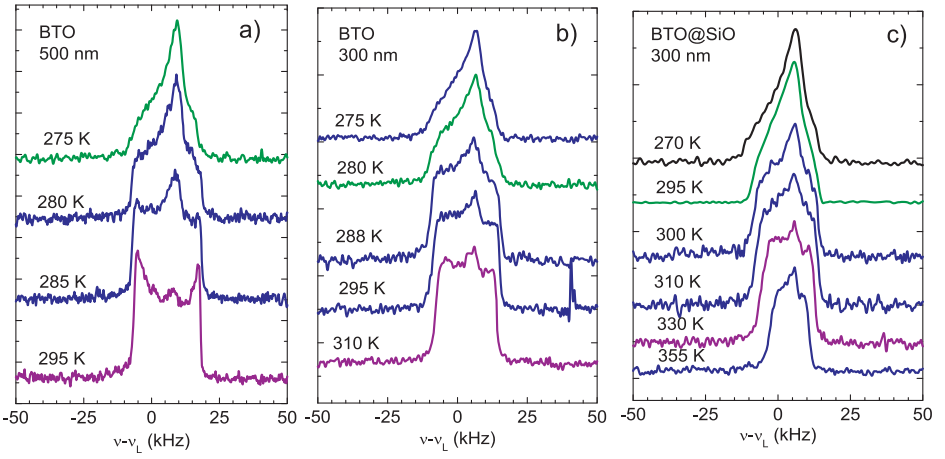

Figure 3. ^{137}Ba NMR spectra measured in vicinity of the tetragonal-orthorhombic phase transition in $BaTiO_3$ powder with particle sizes (a) 500 and (b) 300 nm and (c) in BTO-300@SiO_2 ceramics.

with particle size 300 and 500 nm and BTO-300@SiO_2 ceramics contains the same very narrow line (the linewidth is only 250−300 Hz) at the Larmor frequency in the paraelectric cubic phase at $T = 393-403$ K. It indicates that the electric field gradients are small enough or zero. Therefore, even smallest particles have undistorted cubic perovskite structure and all changes in the spectrum with temperature are exclusively related to phase transitions and influence of surface stresses and depolarizing fields [4] on the phase transitions. It should be, however, noted that while in the micrograin ceramics (Figure 4(a)), the phase transition is sharp, as is expected for the phase transition of the first order, for small $BaTiO_3$ particles this transition is smeared at temperature and is shifted to lower temperature by about 10 deg. It realizes between 383−387 K (Figure 4(c)). But contrary, it seems that the phase transition to the cubic phase is shifted to higher temperature in the core-shell composition. Here, the spectrum becomes narrow only at about 403 K (Figure 4(d)) indicating that the ferroelectric phase completely disappears only above 403 K, 10 deg. higher than the temperature in bulk material. Below we provide detailed analysis of NMR lineshapes to prove our qualitative consideration.

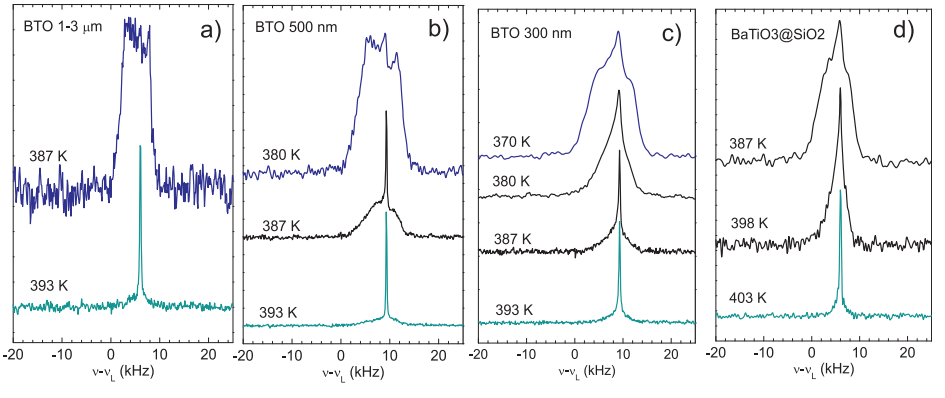

Figure 4. ^{137}Ba NMR spectra measured in vicinity of the cubic-tetragonal phase transition in (a) bulk ceramics, (b) BTO-500 and (c) BTO-300 powders and (d) BTO-300@SiO_2 ceramics.

3.3. *Analysis of the NMR spectra*

Measured NMR spectra correspond to the $1/2 \leftrightarrow -1/2$ central transition perturbed by the second-order quadrupole interaction of the ^{137}Ba nuclei with electric field gradients. Its frequency shift is usually described by the following relation [13]:

$$\nu - \nu_L = \frac{9I(I+1) - 3/4}{16[2I(2I-1)]} \cdot \frac{C_q^2}{\nu_L} f(\theta, \varphi, \eta), \tag{1}$$

where $C_q = \frac{e^2qQ}{h}$ is the nuclear quadrupole coupling constant, $eq \equiv V_{zz}$ is the largest EFG component, Q is the quadrupole moment of a nucleus, the function $f(\theta, \varphi, \eta)$ describes angular variations of the NMR frequency and $\eta = (V_{xx} - V_{yy})/V_{zz}$ is the EFG asymmetry parameter.[13] For powdered or ceramic samples, the frequency shift has to be averaged over all random orientations of particles.

The NMR lineshapes were simulated with the Bruker program 'Powder' to obtain values of the nuclear quadrupole coupling constant and the asymmetry parameter η. The simulated spectra together with the measured ones are presented in Figure 5 for the temperatures which correspond to the tetragonal and orthorhombic phases of bulk $BaTiO_3$. In the orthorhombic phase at $T = 275$ K, the lineshape of the three BTO samples (BTO-500 nm, BTO-300 nm and BTO-300@SiO_2) is well fit by only one spectral component with approximately the same parameters of EFG tensor: $C_q = 2.10$ MHz and $\eta = 0.9$ that correspond to pure orthorhombic phase of bulk $BaTiO_3$.[12] On the other hand, at the

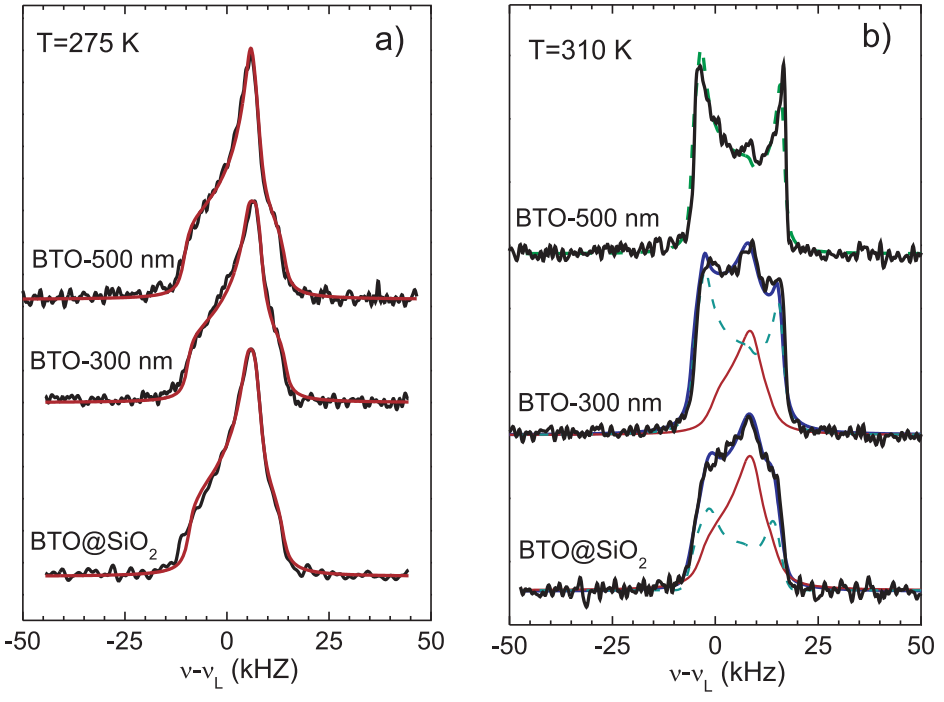

Figure 5. Measured (black lines) and simulated ^{137}Ba NMR spectra in (a) orthorhombic and (b) tetragonal phases of $BaTiO_3$. Smooth lines are the simulated spectra. The thin solid and dashed lines in graph (b) show contributions from regions with the orthorhombic and tetragonal symmetries, respectively. The orthorhombic symmetry phase dominates in BTO-300@SiO_2.

temperature 310 K, in the formal tetragonal phase, only the spectrum of BTO with the largest particle size (500 nm) can be well described by one component with the EFG parameters $C_Q = 2.85$ MHz and $\eta = 0$, which are close to those in bulk material.[12]

For smaller particles (BTO-300 nm) and the BTO-300@SiO_2 core-shell ceramics, the lineshape is composed from two components: one component corresponds to the contribution from the regions with the tetragonal symmetry and the second one corresponds to the regions with the orthorhombic symmetry of EFG tensors. The second component with orthorhombic symmetry of the EFG tensor even dominates in the BTO-300@SiO_2 compound at 310 K in the nominal tetragonal phase. We should here emphasize that the present spectra can be also formally simulated assuming the presence of cubic symmetry component instead of the orthorhombic one as was done in [14,15] for $BaTiO_3$ nanopowders with particle size from 15 to 155 nm. This component with average cubic symmetry, but broadened by random distortions of lattice, is assumed to originate from near-surface regions of nanoparticles, where the polar phase is suppressed. But, as we will show below, this second component in our spectra manifests distinct changes with temperature that clearly supports its polar non-cubic origin. In particular, it narrows to the value expected for the non-polar cubic phase at the temperature 403 K (Figure 4(d)). Besides, the NMR spectrum of BTO-300@SiO_2 core-shell ceramics in the paraelectric phase is identical to the spectrum in bulk material that excludes visible contribution of near-surface regions with non-cubic symmetry as particles are rather large.

The decomposition of NMR lineshape at two components at different temperatures is shown in Figure 6 for BTO-300@SiO_2 ceramics. Temperature dependence of the intensities of the tetragonal and orthorhombic symmetry components is presented in Figure 7 as a phase diagram. This phase diagram contains also data for the low-temperature orthorhombic-rhombohedral phase transition, which we will discuss in the next section. One can see that the tetragonal symmetry phase smoothly increases in volume when the temperature increases from 300 up to 330 K. Then it decreases and completely disappears around 380 K. At higher temperatures, only the orthorhombic symmetry phase exists in the whole volume of sample. This phase transforms into the paraelectric cubic phase at 400−403 K where the spectrum becomes extremely narrow, characteristic feature of perfect cubic structure (see Figure 6, lowermost spectrum). One can thus conclude that mechanical stresses in grains from the dielectric shell stabilize the orthorhombic-like symmetry phase. However, its actual space group can differ from *C2mm*. NMR does not allow to distinguish different space groups belonging to orthorhombic crystal system. Obviously, the mechanical stresses in grains between particles in BTO-300@SiO_2 ceramics are not isotropic, hydrostatic-like, which usually decreases stability of ferroelectric phase.[4] On the other hand, anisotropic stress and surface charges can increase stability of ferroelectric phase. Therefore, ferroelectric phase exists at higher temperature in BTO-300@SiO_2 ceramics as compared to bulk $BaTiO_3$ ceramics. Similar results were obtained in [9] for BTO-50@Al_2O_3 core-shell ceramics with particle size of only 50 nm. In these ceramics, the paraelectric-ferroelectric phase transition was observed at 390 K. Of course, for single nanoparticles, especially of spherical shape, the temperature of phase transition decreases as compared to bulk material, similarly exposed to hydrostatic pressure.[3,4]

3.4. Orthorhombic-rhombohedral phase transition

3.4.1. EPR data

At first, we applied EPR technique to detect the low-temperature orthorhombic-rhombohedral phase transition. Previous EPR studies of bulk $BaTiO_3$ in the form of single

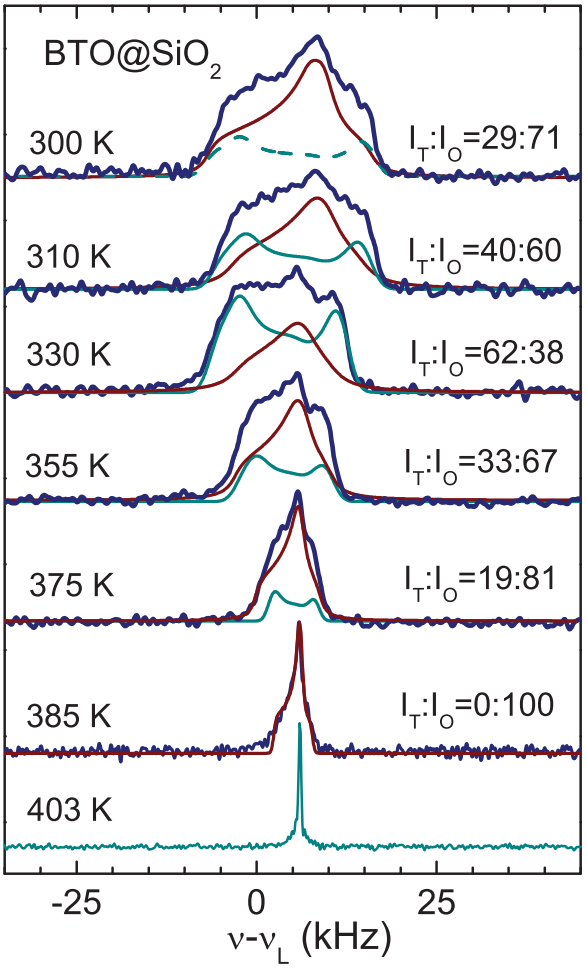

Figure 6. Temperature dependence of ^{137}Ba NMR spectra in BTO-300@SiO_2 ceramics and their simulation (thin lines) at selected temperatures showing change of tetragonal and orthorhombic symmetry contributions to the NMR spectrum with temperature in the temperature region 300−385 K. For comparison, the spectrum in the cubic phase at $T = 403$ K is shown as well.

crystals and ceramics have shown that the EPR spectra of the Mn^{2+} and Fe^{3+} impurity ions are strongly sensitive to crystal structure transformation in $BaTiO_3$.[16,17] These paramagnetic ions were exploited in study of $BaTiO_3$ nanoparticles as well, but only at T > 296 K.[15,18,19] We used this opportunity to detect the orthorhombic-rhombohedral phase transition in nanoparticles and BTO@SiO_2 ceramics. Our samples were not specially doped by paramagnetic ions. They were presented in samples with the concentration from few ppm up to 10−20 ppm as a background impurities.

As the reference, first we measured EPR spectra in the vicinity of the orthorhombic-rhombohedral phase transition in the normal bulk ceramic sample. The spectra of both paramagnetic ions are very broad and thus practically invisible in the orthorhombic phase (Figure 8(a)) due to large zero-field splitting of the $S = 5/2$ spin levels. However, the spectral lines become narrow and strong in the rhombohedral phase at T < 182 K as the local symmetry of the crystal field at positions of the paramagnetic ions is almost cubic in

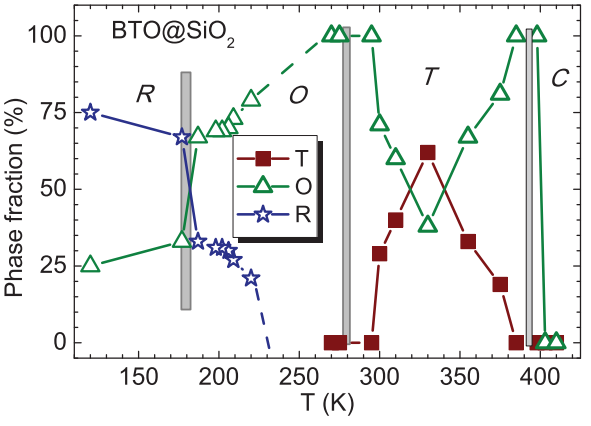

Figure 7. Phase diagram of BTO-300@SiO_2 ceramics obtained on the base of ^{137}Ba NMR spectra analysis. Vertical columns show temperature regions of the tetragonal-cubic, orthorhombic-tetragonal and orthorhombic-rhombohedral phase transitions in bulk material. Actual space group of the orthorhombic-like fraction in the vicinity of the *T*-C phase transition and in the rhombohedral phase can differ from the orthorhombic *C2mm* crystal symmetry.

this phase (see, e.g. [16]). This is due to the fact that paramagnetic ions do not exactly follow the shift of Ti ions at the orthorhombic-rhombohedral phase transition.[16] They incorporated in the oxygen octahedron of the $BaTiO_3$ in a more centred position than Ti^{4+}.

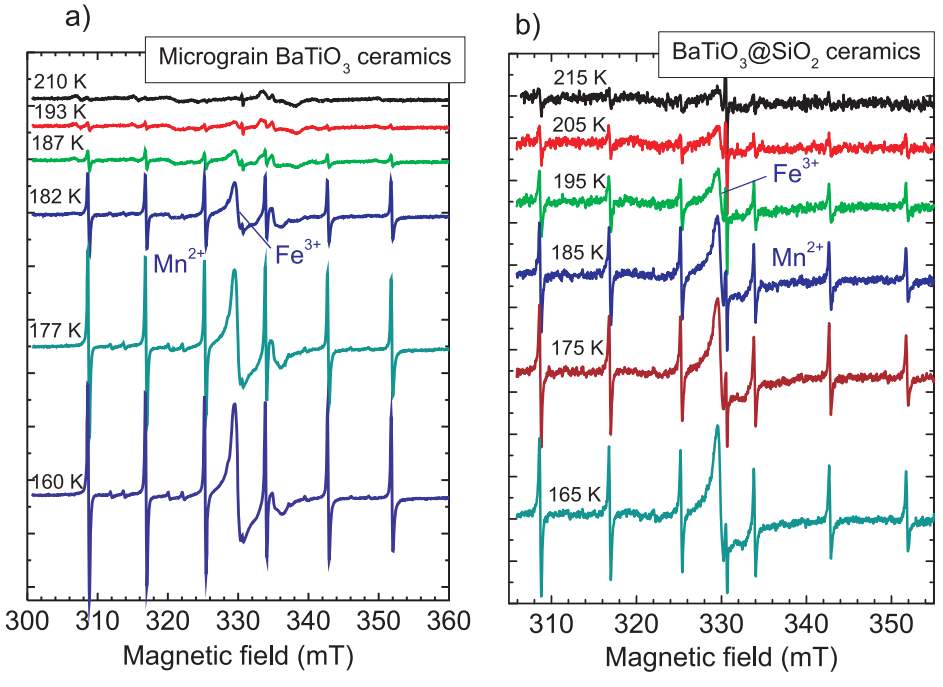

Figure 8. EPR spectra of Mn^{2+} (six-line spectrum) and Fe^{3+} (single line) in (a) micrograin $BaTiO_3$ ceramics and (b) BTO-300@SiO_2 ceramics measured on cooling.

One can see (Figure 8(a)) that EPR spectra of both paramagnetic ions in the micrograin ceramics sharply increase in intensity between 187 and 182 K indicating on the onset of the rhombohedral phase at T < 182 K. In BTO-300@SiO_2 ceramics, EPR spectra start to appear already at 215 K (Figure 8(b)) indicating that the rhombohedral phase appears at much higher temperature as compared to bulk material.

Because EPR intensity is proportional to the volume of the rhombohedral phase in sample, in Figure 9(a) we plot normalized EPR intensity of Mn^{2+} (we accounted change of EPR intensity due to the Boltzmann '1/T' factor) as a function of temperature for three samples: micrograin ceramics, BTO-300 nm nanopowder and core-shell ceramics. The phase transition is sharp in normal micrograin ceramics in accordance with the first order phase transition. It undergoes at the temperature interval expected for bulk material, shown by the vertical column in the graph. But it becomes diffusive for nanoparticles and core-shell ceramics. Moreover, it is shifted to lower temperature for the smallest nanoparticles, but for core-shell ceramics the shift is in opposite direction, the temperature of phase transition increases by almost 25 deg. The same shift of the phase transition takes place in BTO core-shell ceramics with aluminum oxide shell (Figure 9(b)). This graph also demonstrates temperature hysteresis at the phase transition which is, nevertheless, markedly smaller than that in bulk material. Such changes are not only related to the distribution of particle size but also to mechanical surface stresses which can partially change the type of the phase transition from the first order to second order similarly as under the influence of high hydrostatic pressure.[20]

3.4.2. NMR data

Unfortunately, the actual symmetry of the low-temperature phase cannot be determined from EPR data as the paramagnetic ions do not exactly follow the shifts of host ions. EPR spectrum reflects only local symmetry at site of paramagnetic ion location. This symmetry is almost cubic in the rhombohedral phase from the point of view of EPR. Therefore, we measured NMR spectra of ^{137}Ba isotope at temperature 120−220 K, which reflect, at least, true symmetry of EFG tensor at Ba ion position. Such data are presented in Figure 10 for the core-shell ceramics. In contrast to EPR, NMR allows us to see a spectrum at the same intensity in both the orthorhombic and rhombohedral phases. At the

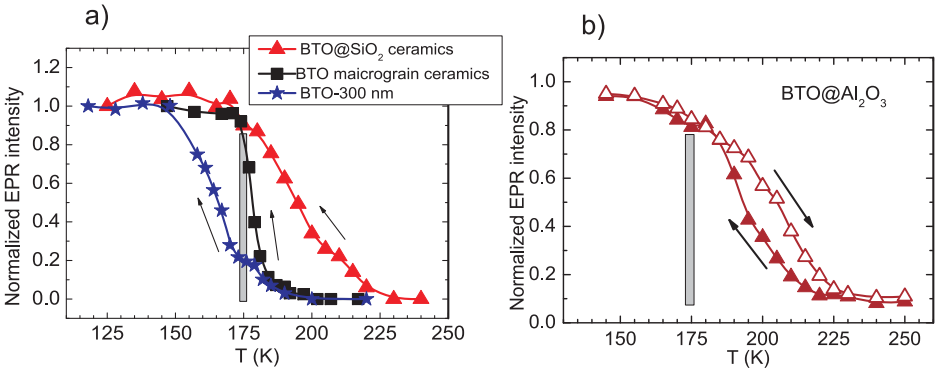

Figure 9. (a) Temperature dependencies of Mn^{2+} EPR intensity at the orthorhombic-rhombohedral phase transition measured at cooling for BTO micrograin ceramics, BTO-300 powder and BTO-300@SiO_2 ceramics. Graph (b) demonstrates the temperature hysteresis at the orthorhombic-rhombohedral phase transition in BTO-300@Al_2O_3 ceramics. The grey vertical columns show temperature region of the phase transition in bulk material, on cooling.

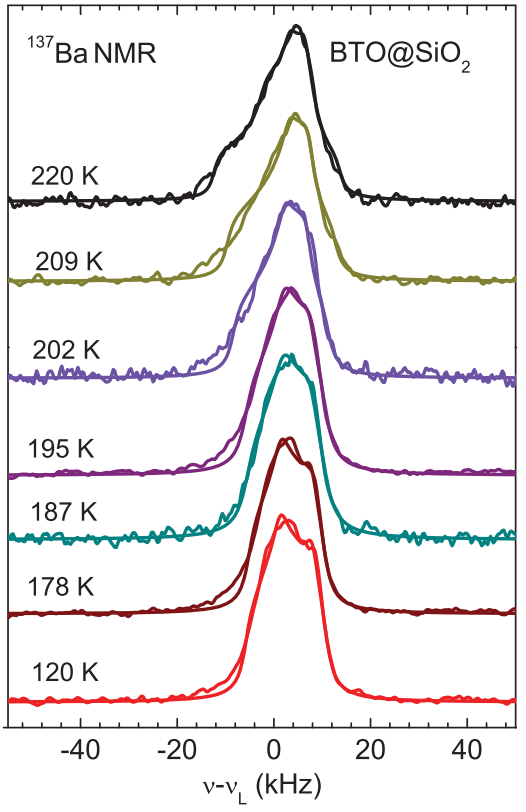

Figure 10. ^{137}Ba NMR spectra measured in the vicinity of the orthorhombic-rhombohedral phase transition in BTO@SiO_2 ceramics. Smooth solid lines are simulated spectra.

phase transition, the symmetry of EFG tensor at Ba position has to change from the orthorhombic to cylindrical (tetragonal). This means that the parameter of asymmetry η of the EFG tensor has to decrease to zero in the low-temperature rhombohedral phase. One can see (Figure 10) that the NMR spectrum really changes the shape at the phase transition. The measured spectra are well simulated assuming general orthorhombic symmetry of EFG tensor. The value of one of the simulation parameters, namely the EFG asymmetry parameter η, as a function of temperature is shown in Figure 11. It undergoes distinct change at the phase transition. However, it does not decrease completely to zero as it should be in pure rhombohedral phase. Therefore, the symmetry of the low-temperature phase is not pure rhombohedral. It contains probably a residual of the orthorhombic symmetry phase. For comparison, Figure 11 shows also change of the asymmetry parameter in the initial BTO-300 nm powder. Similar to EPR data, the phase transition is shifted to higher temperature in the core-shell ceramic sample as compared to the initial powder or bulk material.

4. Discussion

It is well known that the temperature of phase transition of an isolated ferroelectric particle depends on its size because the surface of a particle acts as a hydrostatic pressure. This phenomenon is well understood in the phenomenological approach where the free

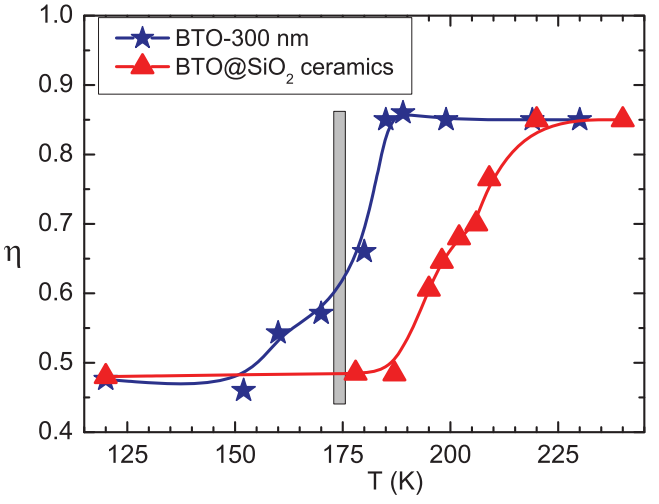

Figure 11. Temperature dependence of EFG asymmetry parameter in BTO-300 powder and $BTO@SiO_2$ ceramics determined from analysis of ^{137}Ba NMR spectra in the vicinity of the orthorhombic-rhombohedral phase transition. The grey vertical column shows temperature region of the phase transition in bulk material, on cooling.

energy functional contains surface energy expressed via surface tension. The detailed consideration of this theory is presented, for example, in publication.[4] In this approach, the temperature of the paraelectric-ferroelectric phase transition is function of the particle radius. It can be expressed as [4]

$$T_C(R) \approx T_C\left(1 - \frac{R_{CR}(0)}{R}\right), \tag{2}$$

where $T_C = 393$ K is the temperature of the paraelectric-ferroelectric phase transition in bulk $BaTiO_3$, $R_{CR}(0) = 9-12$ nm is the critical radius of $BaTiO_3$ particle at 0 K. The critical radius depends on temperature. At room temperature, it is about 40 nm for $BaTiO_3$. For our particles with average diameter of 300 nm, the expected temperature of the phase transition is around 370−375 K, 10 deg. lower than determined by us experimentally. There is a reasonable agreement between theory and experiment taking into account proximity of the formula (2) and, more importantly, the non-spherical shape of particles, their distribution in size. For instance, not only compressive stress but also shear stress should be accounted for.

From the shift of the phase transition temperature in BTO-300 nm nanoparticles, we can also estimate equivalent hydrostatic pressure which shifts the phase transition to the same temperature. It is known from experiment [21,22] that the temperature of the cubic-tetragonal phase transition linearly decreases with increasing pressure with a slope of -5.8×10^{-3} deg./atmos. For our particles, this equivalent compressive pressure is large enough, about 3000 atm.

Let us discuss the results obtained for the core-shell ceramic compound. In Figure 7, the phase diagram of the core-shell compound is extended to the low-temperature rhombohedral phase. It was pointed out above that NMR lineshape at temperatures lower than 220 K cannot be described by EFG tensor of cylindrical symmetry valid for the rhombohedral symmetry, as here there is a mixing of two phases. We have performed decomposition of NMR spectrum at the temperature region of the orthorhombic-rhombohedral phase

transition into two components: one corresponds to the contribution of orthorhombic symmetry phase; and the second one, contribution of the rhombohedral symmetry phase. These data are presented in Figure 7 as phase fractions. One can see that there is a wide temperature region (120−230 K) where both phases coexist one with other. Moreover, the phase with rhombohedral symmetry is extended up to about 230 K. This is in good agreement with EPR, which also detects the rhombohedral phase at the temperature far from the temperature of phase transition in bulk material. However, the abrupt change of the ratio between volumes of phases at 175−180 K indicates phase transition, as in bulk material, at least in half of the material volume.

Coexistence of different structural phases was recently reported for $BaTiO_3$ nanopowders with average sizes of particles from 5 to 100 nm by using high resolution synchrotron diffraction technique.[8] These results are in qualitative agreement with our results. In particular, it was reported that the orthorhombic phase coexists with other phases at the temperatures from 200 up to 450 K. In BTO@SiO2 nanocomposite ceramics, the phase with the orthorhombic symmetry of EFG tensor was detected in all three polar phases. It completely disappears only above 400 K, where it transforms into the cubic phase. Volume of this phase changes at all phase transitions. Therefore, we can conclude that the most stable structural phase in BTO core-shell nanostructure is the phase with orthorhombic-like symmetry. Obviously, it is stabilized by anisotropic components of surface stresses such as shear stress near surface boundaries of particles in the core-shell structure or even in a single nanoparticle. There is always a competition between compressive and shear stresses. This conclusion is in line with the results obtained in [9] for BTO-50@Al_2O_3 core-shell ceramics with particles size of about 50 nm. The Curie transition temperature in this ceramics is 390 K, while it has to be below room temperature in accordance with Equation (2).

Finally, we note that all these surface effects become important only in the vicinity of phase transitions where lattice is soft and extremely sensitive to external influences as no change of cubic perovskite structure is seen in the paraelectric phase of the BTO core-shell nanostructure excepting obviously few atomic layers near surface of a particle.

5. Conclusion

We studied the lattice structure transformations in nanopowders of classical ferroelectric $BaTiO_3$ and BaTiO3@SiO_2 core-shell nanostructured ceramics using NMR and EPR techniques. Our main finding is that even in relatively large particles of $BaTiO_3$, with average size of 300 nm, there is marked influence of mechanical surface stresses on lattice parameters in vicinity of phase transitions, especially at the low-temperature orthorhombic-rhombohedral phase transition. The influence of the surface stresses (stresses at surface boundaries in grains) is essentially stronger in the core-shell nanostructured ceramics as compared to single particles.

The most exciting result is that there is a coexistence of adjacent ferroelectric phases in wide temperature regions even in nanocompound with relatively large ferroelectric particles. The most stable is the orthorhombic-like symmetry phase which coexists with other polar phases in the core-shell nanostructured ceramics in the temperature interval that includes all polar phases of $BaTiO_3$. It transforms into the cubic paraelectric phase only at $T > 400-403$ K, almost 10 deg. higher than the phase transition temperature in bulk material. We note that the actual space group of the orthorhombic symmetry phase can differ from *C2mm* at temperatures where it coexists with other phases as NMR, alone, does not allow us to distinguish different space groups belonging to orthorhombic crystal

system. It could be, for instance, even monoclinic *Pm* and *Cm* space groups recently proposed in $KNbO_3$ and $BaTiO_3$ nanowires instead of *R3m* rhombohedral phase.[23]

Our results suggest that besides compressive surface tension, anisotropic stresses like shear stress can be dominated in the core-shell nanostructures. They can essentially increase stability of ferroelectric phase.

Disclosure statement

No potential conflict of interest was reported by the authors.

Funding

The research was in part supported by the GA CR [grant number 13-11473S].

References

[1] Jona F, Shirane G. Ferroelectric crystals. 2nd ed. Mineola: Dover Publications; 1993.

[2] Shebanov LA. X-ray temperature study of crystallographic characteristics of Barium titanate. Phys Stat Solidi (a). 1981;65:321–325.

[3] Wang YG, Zhong WL, Zhang PL. Size driven phase transition in ferroelectric particles. Solid State Comm. 1994;90:329–332.

[4] Glinchuk MD, Morozovskaya AN. Effect of surface tension and depolarization field on ferroelectric nanomaterial properties. Phys Stat Solidi (b). 2003;238:81–91.

[5] Schlag S, Eicke H-F. Size driven phase transition in nanocrystalline $BaTiO_3$. Solid State Comm. 1994;91:883–887.

[6] Tsunekawa S, Ito S, Mori T, Ishikawa K, Li Z-Q, Kawazoe Y. Critical size and anomalous lattice expansion in nanocrystalline $BaTiO_3$ particles. Phys Rev B. 2003;62:3065.

[7] Uchino K, Sadanaga E, Hirose T. Dependence of the crystal structure on particle size in barium titanate. J Am Ceram Soc. 1989;72:1555–1558.

[8] Zhu J, Han W, Zhang H, Yuan Z, Wang X, Li L. Phase coexistence evolution of nano BaTiO3 as function of particle sizes and temperatures. J Appl Phys. 2012;112:064110.

[9] Aymonier C, Elissalde C, Reveron H, Weill F, Maglione M, Cansell F. Supercritical fluid technology of nanoparticle coating for new ceramic materials. Nanosci Nanotechnol. 2005;5:980–983.

[10] Hornebecq V, Huber C, Maglione M, Antonietti M, Elissalde C. Dielectric properties of pure (BaSr)TiO3 and composites with different grain sizes ranging from the nanometer to the micrometer. Adv Funct Mater. 2004;14:899–904.

[11] Huber C, Elissalde C, Hornebecq V, Mornet S, Treguer-Delapierre M, Weill F, Maglione M. Nano-ferroelectric based core–shell particles: towards tuning of dielectric properties. Ceramics Int. 2004;30:1241–1245.

[12] Bastow TJ, Whitfield HJ. ^{137}Ba and ^{47,49}Ti NMR: electric field gradients in the non-cubic phases of BaTiO3. Solid State Commun. 2001;117:483–488.

[13] Abragam A. Principles of nuclear magnetism. New York (NY): Oxford University Press; 1961.

[14] Erdem E, Bottcher R, Glasel H-J, Hartmann E, Lotzsche G, Michel D. Size effects in $BaTiO_3$ nanopowders studied by EPR and NMR. Ferroelectrics. 2005;316:43–49.

[15] Glasel H-J, Hartmann E, Hirsch D, Bottscher R, Klimm C, Michel D, Semmelhack H-C, Hormes J, Rumpf H. Preparation of barium titanate ultrafine powders from a monomeric metallo-organic precursor by combined solid-state polymerisation and pyrolysis. J Mat Sci. 1999;34:2319–2323.

[16] Siegel E, Muller KA. Structure of transition-metal–oxygen-vacancy pair centers. Phys Rev. B. 1979;19:109.

[17] Milsch B. Evaluation of lattice site and valence of manganese in polycrystalline $BaTiO_3$, and n-$BaTiO_3$, by electron paramagnetic resonance. Phys Stat Solidi (a). 1992;133:455–464.

[18] Bottcher R, Klimm C, Michel D, Semmelhack H-C, Volkel G, Glasel H-J, Hartmann E. Size effect in Mn^{2+}-doped $BaTiO_3$ nanopowders observed by electron paramagnetic resonance. Phys Rev. B. 2000;62:2085−2095.
[19] Glinchuk MD, Kondakova IV, Slipenyuk AM, Laguta VV. Investigation of ferroelectric nanopowders by EPR method. Phys Stat Solidi (c). 2007;4:1297−1300.
[20] Decker DL, Huang Ke, Nelson HM. Electron paramagnetic resonance measurements near the tricritical point in $BaTiO_3$. Phys Rev. B. 2002;66:174103.
[21] Merz WJ. The effect of hydrostatic pressure on the curie point of barium titanate single crystals. Phys Rev. 1950;77:52.
[22] Schirane G, Takeda A. Transition energy and volume change at three transitions in barium titanate. J Phys Soc Japan. 1952;7:1−4.
[23] Louis L, Gemeiner P, Ponomareva I, Bellaiche L, Geneste G, Ma W, Setter N, Dkhil B. Low-symmetry phases in ferroelectric nanowires. Nano Lett. 2010;10:1177−1183.